Engineering Structures 61 (2014) 153–165

Contents lists available at ScienceDirect

Engineering Structures

journal homepage: www.elsevier.com/locate/engstruct

Damage assessment of adjacent buildings under earthquake loads

Abbas Moustafa [a], Sayed Mahmoud [b,c,*]

[a] Department of Civil Engineering, Faculty of Engineering, Minia University, Minia 61111, Egypt
[b] Department of Civil Engineering, Faculty of Engineering at Rabigh, King Abdulaziz University, Saudi Arabia
[c] Faculty of Engineering at Mataria, Helwan University, Egypt

ARTICLE INFO

Article history:
Received 6 May 2013
Revised 26 December 2013
Accepted 6 January 2014
Available online 7 February 2014

Keywords:
Adjacent buildings
Base-isolation
Damage index
Ductility
Earthquake loads
Inelastic structures

ABSTRACT

This paper deals with damage assessment of adjacent colliding buildings under strong ground motion. In previous studies, the structure input-response pair is used to examine pounding effects on adjacent buildings under seismic loads. In this paper, pounding of adjacent buildings is assessed using input energy, dissipated energy and damage indices. Damage indices (DI) are computed by comparing the structure's responses demanded by earthquakes and the associated structural capacities. Damage indices provide quantitative estimates of structural damage level, and thus, a decision on necessary repair can be taken. Adjacent buildings with fixed-base and isolated-base are considered. The nonlinear viscoelastic model is used for capturing the induced pounding forces. Influences of the separation distance between buildings, buildings properties, such as, base-condition (fixed or isolated), and yield strength on damage of adjacent buildings are investigated. The set of input ground motions includes short-, moderate- and long-duration accelerograms measured at near-fault and far-fault regions with different soil types. Earthquake records with different characteristics are considered to study damage of adjacent buildings under seismic loads. Numerical illustrations on damage of fixed-base and isolated-base adjacent buildings with elastic–plastic force–deformation relation are provided.

1. Introduction

The unexpected severe damage of infrastructure and buildings and the loss of lives during recent earthquakes (e.g., 12 January 2010 Haiti earthquake and 11 March 2011 Tohoku Japan earthquake) as well as previous earthquakes, such as, 1994 Northridge and 1995 Kobe earthquakes, have raised significant concern and questions on life safety and performance of engineering structures under possible future earthquakes [1]. Yet, earthquakes continue to claim thousands of lives and to damage structures worldwide every year [2]. The occurrence of strong motion earthquakes in densely populated regions, especially in developing countries with a vulnerable buildings stock and fragile infrastructure, could lead to catastrophic consequences. A notable example is the 12 January 2010 Haiti earthquake that killed 250,000 people and left a long-term suffering for residents of this country [3]. Furthermore, the 11 March 2011 Japan earthquake has caused severe destruction to engineering structures and critical facilities in one of the most developed countries in the world, emphasizing serious challenges facing the earthquake engineering community [4]. Hence, the assessment of seismic performance of structures under strong ground motions represents an important problem in earthquake engineering. Structures need to resist possible future earthquakes which add more complexity to the problem [5]. The consideration of the earthquake characteristics and the structural inelastic behavior is essential for the accurate prediction of the structure response under seismic loads [6].

In heavily populated regions and Mega cities, such as Cairo and Jeddah, buildings are constructed side by side without separation distances. This, in turn, could cause pounding of adjacent structures under earthquake loads. Mathematically, a coupling force appears in the equations of motion of both structures. This phenomenon has been observed during the 12 October 1992 Dahshur earthquake (M 5.6, 561 deaths and 10,000 injuries) in the Greater Cairo area [7]. A significant attention to this phenomenon has been paid after the 19 September 1985 Mexico earthquake in which about 40% of the collapsed or severely damaged buildings have experienced some level of pounding and in 15% of them pounding led to total collapse [8]. Pounding of adjacent structures has been extensively studied during the last two decades or so. Comprehensive reviews of literature on this subject can be found in Refs. [9–17]. Pounding occurs to adjacent structures due to the difference

* Corresponding author at: Department of Civil Engineering, Faculty of Engineering at Rabigh, King Abdulaziz University, Saudi Arabia. Tel./fax: +966546884922.
E-mail addresses: abbas.moustafa@mu.edu.eg (A. Moustafa), elseedy@hotmail.com (S. Mahmoud).

http://dx.doi.org/10.1016/j.engstruct.2014.01.004
0141-0296/

of their dynamic properties and the insufficient separation distance between them. Structural pounding can be modeled using elastic and inelastic structural models. In the first case, the structures' deformations do not exceed the elastic limit, and thus, damage does not occur. In the second case, the deformations are composed of an elastic recoverable part and an inelastic unrecoverable part [18]. In general, buildings are idealized as single-degree-of-freedom (SDOF) systems or multi-degree-of-freedom (MDOF) systems (e.g., [19–21]). Lumped mass models and continuous beam models have been used to idealize the pounding arising in adjacent buildings under ground accelerations (see, e.g., [22–25]). Nonlinear response of adjacent buildings has been studied by Athanassiadou and Penelis [26]. Anagnostopoulos [9] presented a comprehensive study on pounding of adjacent buildings modeled as SDOF nonlinear systems. Pantelides and Ma [27] considered the coupling behavior of damped SDOF elastic and inelastic structures with one-sided pounding during earthquakes using the Hertz contact model. Muthukumar and Des Roches [28] studied pounding of adjacent structures modeled as elastic and inelastic SDOF systems using different pounding models. Jankowski [29] proposed the notion of the impact force response spectrum for elastic and inelastic adjacent structures. Pounding of structures modeled as MDOF systems has also been investigated in several studies (see, e.g., [30]). In a previous paper, the seismic response of adjacent buildings supported on different or similar base systems (fixed-base and isolated-base) considering impacts between the bases and the superstructures have been numerically investigated [11,31,32].

In general, the coupling effect of adjacent buildings under earthquake loads is investigated by comparing the input ground motion and the associated structural response. This paper investigates damage of adjacent buildings with fixed-base and isolated-base under strong ground motion. Damage of inelastic buildings is quantified in terms of damage indices and hysteretic energy dissipated by inelastic deformations. The next section provides a brief overview on damage quantification in structures under earthquake loads using damage indices. Section 3 demonstrates pounding models of adjacent inelastic buildings with fixed-base and isolated-base. Section 4 describes the system parameters for fixed-base and isolated-base adjacent buildings. The set of strong ground motions used as input to adjacent structures and the response quantities are defined in the same section. Section 5 provides numerical illustrations on the formulation developed in this paper. Section 6 presents the main conclusions drawn based on the numerical results achieved in this study.

2. Damage measures of structures under earthquake loads

A vast research has been carried out on damage of structures under strong ground motion. Moustafa [5] provided a comprehensive review on the literature of this subject. A brief review is presented here for the sake of completeness.

The literature on damage measures of structures under strong ground motions is vast (e.g., [33–38]). Damage indices are based on either a single or a combination of structural response parameters. Ref. [5] summarizes several damage measures that are based on a single or multiple response parameters [34,39]. The first measure indicates the ultimate ductility produced during the ground shaking (the ratio of the maximum absolute displacement demanded by the earthquake and the yield displacement). Clearly, this measure does not incorporate any information on how the earthquake input energy is imparted on the structure nor how this energy is dissipated. Earthquake damage occurs not only due to the maximum deformation or ductility but is associated with the hysteretic energy dissipated by the structure as well. The definition of structural damage in terms of the ductility factor is therefore inadequate. Three measures indicate the rate of the earthquake input energy to the structure (i.e., how fast the input energy is imparted by the earthquake and how fast it gets dissipated).

Damage indices can be estimated by comparing the response parameters demanded by the earthquake with the structural capacities. Powell and Allahabadi [39] proposed a damage index in terms of the ultimate ductility (capacity) μ_u and the maximum ductility (demand) attained during ground shaking $\mu_{\max}$:

$$DI_{AP} = \frac{x_{\max} - x_y}{x_u - x_y} = \frac{\mu_{\max} - 1}{\mu_u - 1} \tag{1}$$

However, DI_{AP} does not include effects from hysteretic energy dissipation. Fajfar [33] and Cosenza et al., [34] proposed a damage index based on the structure hysteretic energy E_H, given as:

$$DI_{FC} = \frac{E_H/(f_y x_y)}{\mu_u - 1} \tag{2}$$

where f_y, x_y, E_H are the yield strength, yield displacement, and hysteretic energy, respectively (Section 4.3 demonstrates the estimation of the earthquake input energy to the structure and associated energies dissipated by the structure). A robust damage measure should include not only the maximum response but the effect of repeated cyclic loading as well. Park and co-workers developed a simple damage index, given as [40–42]:

$$DI_{PA} = \frac{x_{\max}}{x_u} + \gamma \frac{E_H}{f_y x_u} = \frac{\mu_{\max}}{\mu_u} + \gamma \frac{E_H}{f_y x_y \mu_u} \tag{3}$$

Here, $x_{\max}$, E_H are the maximum displacement and dissipated hysteretic energy (excluding elastic energy) under the earthquake. Note that $x_{\max}$ is the maximum absolute value of the displacement response under the ground motion. x_u is the ultimate deformation capacity under monotonic loading and γ is a positive constant that weights the effect of cyclic loading on structural damage. Note that $\gamma = 0$ implies that the contribution to DI_{PA} from cyclic loading is omitted.

The state of the structure damage is defined as: (a) repairable damage, when $DI_{PA} < 0.40$, (b) damaged beyond repair, when $0.40 \leqslant DI_{PA} < 1.0$, and (c) total or complete collapse, when $DI_{PA} \geqslant 1.0$. These criteria are based on calibration of DI_{PA} against experimental results and field observations in earthquakes [42]. The Park and Ang damage index reveals that both maximum ductility and hysteretic energy dissipation contribute to the structure resistance during ground motions. In Eq. (3) damage is expressed as a linear combination of the damage caused by excessive deformation and that contributed by repeated cyclic loading effect. Note also that the quantities $x_{\max}$, E_H depend on the loading history while the quantities γ, x_u, f_y are independent of the loading history and are determined from experimental tests.

Another measure of structural performance is given as the dissipated hysteretic energy normalized to the input energy to the structure. Mathematically, this index is given as:

$$DI_H = \frac{E_H}{E_I} \tag{4}$$

The quantification of the energy terms E_H and E_I is provided in Section 4.3. Note that the damage index of Eq. (4) includes the structure's response demanded by the ground motion and the associated structural capacity parameters in an implicit form. Note also that DI_H close to zero implies a linear behavior while DI_H larger than zero indicates inelastic behavior and occurrence of structural damage.

3. Buildings and pounding models

In the present study, idealized mathematical models for adjacent SDOF fixed-base buildings as well as adjacent SDOF isolated-base buildings situated at a gap distance d are considered. To numerically model the pounding phenomenon, a nonlinear spring in conjunction with a nonlinear dashpot element is used for estimating the induced pounding forces acting on the colliding masses.

3.1. Nonlinear buildings model

To assess damage of neighboring buildings insufficiently separated, to allow occurrence of impact, buildings have been idealized as their masses lumped at the floor level, which are considered as rigid in their own plane, assuming that the superstructures to behave in an inelastic way during earthquake excitations. For adjacent base-isolated building structures, the High Damping Rubber Bearings (HDRB), an isolation device, is used in the isolation devices. A nonlinear strain rate dependent model has been adopted to simulate the behavior of HDRB, (see, e.g., [10,43]). This model describes the behavior of the bearing by a nonlinear elastic spring-dashpot element.

3.1.1. Fixed-base buildings

Let m_1, c_1, u_1, r_1 and m_2, c_2, u_2, r_2 be the masses, damping coefficients, displacements and restoring forces for the left and the right buildings, respectively. In the case of two structures with fixed bases (see Fig. 1), the nonlinear dynamic equation of motion can be written as:

$$\begin{pmatrix} m_1 & 0 \\ 0 & m_2 \end{pmatrix}\begin{pmatrix} \ddot{u}_1 \\ \ddot{u}_2 \end{pmatrix}+\begin{pmatrix} c_1 & 0 \\ 0 & c_2 \end{pmatrix}\begin{pmatrix} \dot{u}_1 \\ \dot{u}_2 \end{pmatrix}+\begin{pmatrix} r_1 \\ r_2 \end{pmatrix}+\begin{pmatrix} f_1 \\ -f_1 \end{pmatrix}=-\begin{pmatrix} m_1 & 0 \\ 0 & m_2 \end{pmatrix}\begin{pmatrix} \ddot{u}_g \\ \ddot{u}_g \end{pmatrix} \tag{5}$$

where, $\dot{u}_1$, $\ddot{u}_1$ and $\dot{u}_2$, $\ddot{u}_2$ denote the velocities and accelerations of the left and the right structures, respectively; f_1 is the force due to impact (pounding force); and $\ddot{u}_g$ is the earthquake acceleration. During the elastic stage, the resisting forces, r_1, r_2, take the form: $r_1 = k_1u_1$, $r_2 = k_2u_2$, while during the plastic stage: r_1 varies between f_{y1} and $-f_{y1}$, and r_2 varies between f_{y2} and $-f_{y2}$, where k_1, k_2 and f_{y1}, f_{y2} are the initial stiffness coefficients and yield strength for the left and the right buildings, respectively.

Assuming viscous damping model for both buildings, the values of initial natural period T_i and the damping coefficient c_i ($i = 1, 2$) of the undamaged buildings are given as [44]:

$$T_i=\frac{2\pi}{\omega_i};\quad c_i=2\xi_i\sqrt{k_im_i} \tag{6}$$

Note that $\omega_i=\sqrt{\frac{k_i}{m_i}}$ is the natural frequency of the undamaged structure. The structural response of both buildings is estimated by solving the coupled differential Eq. (5) numerically using the Newmark-Beta method.

3.1.2. Isolated-base buildings

In the case of two base-isolated buildings (see Fig. 2), the nonlinear dynamic equation of motion can be written as

$$\mathbf{M}_i\ddot{\mathbf{U}}_i+\mathbf{C}_i\dot{\mathbf{U}}_i+\mathbf{R}_i+\mathbf{F}_i=-\mathbf{M}_{gi}\mathbf{I}\ddot{u}_g \tag{7a}$$

$$\mathbf{M}_i=\begin{pmatrix} m_i & m_i \\ 0 & m_{bi} \end{pmatrix},\quad \mathbf{M}_{gi}=\begin{pmatrix} m_i & 0 \\ 0 & m_{bi} \end{pmatrix},\quad \mathbf{C}_i=\begin{pmatrix} c_i & 0 \\ -c_i & c_{bi} \end{pmatrix} \tag{7b}$$

$$\mathbf{U}_i=\begin{pmatrix} u_i \\ u_{bi} \end{pmatrix},\quad \dot{\mathbf{U}}_i=\begin{pmatrix} \dot{u}_i \\ \dot{u}_{bi} \end{pmatrix},\quad \ddot{\mathbf{U}}_i=\begin{pmatrix} \ddot{u}_i \\ \ddot{u}_{bi} \end{pmatrix} \tag{7c}$$

$$\mathbf{R}_i=\begin{pmatrix} r_i \\ r_{bi}-r_i \end{pmatrix},\quad \mathbf{F}_1=\begin{pmatrix} f_1 \\ f_{pb1} \end{pmatrix},\quad \mathbf{F}_2=\begin{pmatrix} -f_1 \\ f_{pb2} \end{pmatrix},\quad \mathbf{I}=\begin{pmatrix} 1 \\ 1 \end{pmatrix} \tag{7d}$$

where m_{bi}, u_{bi}, $\dot{u}_{bi}$, $\ddot{u}_{bi}$ ($i = 1, 2$) are the masses, displacements, velocities, and accelerations of the bases of the left and the right buildings, respectively, $r_{bi} = k_{bi}u_{bi}$, k_{bi}, c_{bi} are the resisting forces of the isolation systems, stiffness and damping coefficients for the left and right bases respectively, f_{pbi} is the pounding force due to collisions of the retaining wall and the bases of the left and the right buildings. Furthermore, f_1 is the pounding force arising between the superstructures.

3.2. Nonlinear pounding model

Pounding between adjacent structures is a highly complex phenomenon. Therefore, in order to accurately simulate impact, an appropriate impact force model must be adopted. The nonlinear viscoelastic model [45] which uses the general trend of the nonlinear Hertz law of contact together with an incorporated hysteretic

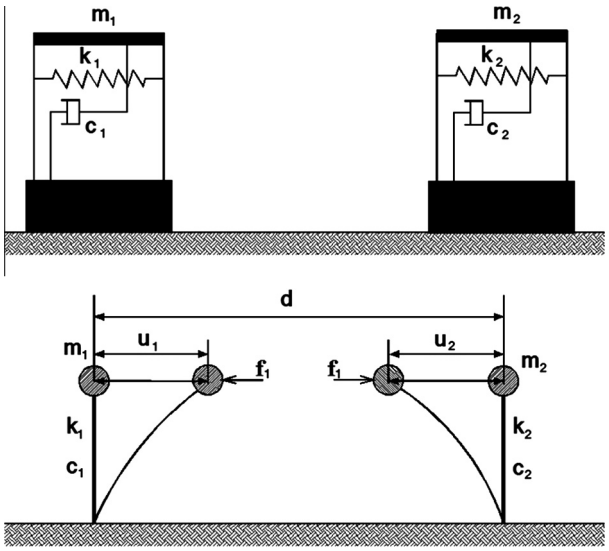

Fig. 1. Colliding model for buildings with fixed bases.

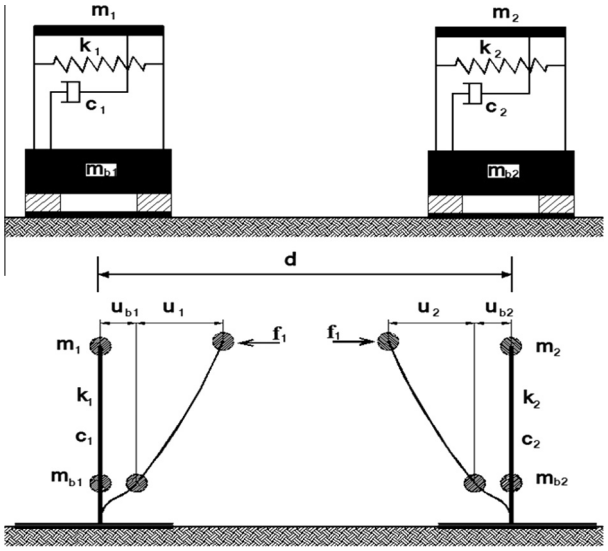

Fig. 2. Colliding model for base-isolated buildings.

damping function simulating the dissipation of energy during impact is utilized to capture impacting force. According to the nonlinear viscoelastic model, the pounding force between two adjacent buildings is given as [45]:

$$\begin{aligned} f_1 &= 0 && \text{for } \delta \le 0 && \text{(no contact)} \\ f_1 &= \bar{\beta}\delta^{\frac{3}{2}} + \bar{c}\dot{\delta} && \text{for } \delta > 0 \text{ and } \dot{\delta}(t) > 0 && \text{(contact-approach period)} \\ f_1 &= \bar{\beta}\delta^{\frac{3}{2}} && \text{for } \delta > 0 \text{ and } \dot{\delta}(t) \le 0 && \text{(contact-restitution period)} \end{aligned}$$

Herein, $\delta = (u_1 - u_2 - d)$ is the relative displacement (d denotes the initial separation gap), $\bar{\beta}$ is the impact stiffness parameter and

$$\bar{c} = 2\bar{\xi}\sqrt{\bar{\beta}\sqrt{\delta}\frac{m_1 m_2}{m_1 + m_2}} \tag{9}$$

is the impact element's damping. Here, $\bar{\xi}$ is an impact damping ratio related to a coefficient of restitution, e which can be defined as [46]:

$$\bar{\xi} = \frac{9\sqrt{5}}{2}\frac{1 - e^2}{e(e(9\pi - 16) + 16)} \tag{10}$$

where e is a constant (typically $e = 0.65$).

4. System parameters and input ground motion

This section defines the parameters of adjacent buildings as well as the set of strong ground motions used as inputs to adjacent buildings. The response quantities used to characterize damage of adjacent buildings are also stated in this section. The details of this information are provided in the following three subsections.

4.1. System parameters

The dynamic parameters of adjacent structures considered in this study are taken from an earlier study by Jankowski [30]. The mass, damping ratio and initial stiffness are taken as 7.5×10^4 kg, 0.05, 1.75×10^6 N/m for the left building and 3.0×10^6 kg, 0.05, 1.32×10^9 N/m for the right building. According to these parameters, one of the two buildings is flexible ($T_n = 1.2$ s) and lighter (left building) while the other building is stiffer ($T_n = 0.3$ s) and heavier (right building). Furthermore, the yield strength for the left and right buildings are taken as $f_{y_l} = 1.369 \times 10^5$ N, and $f_{y_r} = 1.442 \times 10^7$ N, respectively. The base-isolated left building has been equipped with circular HDRBs with the parameters of the bearing's model described in Example 3 of the paper by Jankowski [43]. Furthermore, the base-isolated right building has been equipped with square HDRBs with the parameters of the bearing's model described in Example 1 of the same paper [43]. The numerical values for the parameters of the nonlinear viscoelastic model for the pounding force are taken as $\bar{\beta} = 2.75 \times 10^9$ N/m$^{3/2}$, $\xi = 0.35$ and $e = 0.65$ [30].

4.2. Input ground motion

The set of 12 earthquake ground motion records listed in Table 1 are used in this study as inputs to adjacent buildings. These records are from 1995 Aqaba, 1940 Imperial Valley (El Centro), 1999 Kocaeli, 1989 Loma Prieta, 1994 Northridge, 1995 Kobe, 1999 Chi-Chi, and 1971 San Fernando (Sylmar) earthquakes. The table summarizes important information on these ground motion records, such as, recording station, soil class, magnitude, peak ground acceleration (PGA), site to source distance, total duration and energy (Arias intensity, [47]). These records represent strong ground motion records with different PGA, different frequency content, total duration (15–90 s) and local soil conditions. Fig. 3 depicts the plots for the time-history of the ground acceleration and the associated Fourier amplitude spectrum for each of these records. The earthquake magnitude varies between 6.6 and 7.6 with site-source of about 0.6 to 93.8 km.

4.3. System responses

In this paper, the response of adjacent buildings is assessed in terms of the maximum ductility demand, the pounding force f_1, input and dissipated energies and damage indices of Eqs. (1–4). The input energy to the structure by the earthquake and the associated damping, hysteretic, elastic and kinetic energies dissipated by the structure can be estimated from the energy balance of the equation of motion for the structure (see Eq. (5)) as [48–50]:

$$\begin{aligned} &\int_0^t m_1\ddot{u}_1(\tau)\dot{u}_1(\tau)d\tau + \int_0^t c_1\dot{u}_1^2(\tau)d\tau + \int_0^t r_1(\tau)\dot{u}_1(\tau)d\tau \\ &\quad + \int_0^t f_1(\tau)\dot{u}_1(\tau)d\tau = -\int_0^t m_1\ddot{u}_g(\tau)\dot{u}_1(\tau)d\tau \\ &E_K(t) + E_D(t) + E_S(t) + E_P(t) = E_I(t) \end{aligned} \tag{11}$$

Eq. (11) represents the relative energy terms for the left building. Here $E_I(t)$ is the earthquake relative input energy to the structure since ground starts shaking until it comes to rest. $E_K(t)$ is the relative kinetic energy ($E_K(t) = m_1\dot{u}_1^2(t)/2$) and $E_D(t)$ is the energy absorbed by damping. The energy E_S represents the total relative energy absorbed by the spring and is composed of the recoverable elastic energy and the hysteretic cumulative plastic energy $E_H(t)$. $E_P(t)$ is the energy arising due to the pounding force between the two buildings. Similar energy terms for the right building can be determined from the equation of motion following the same procedures for the right building.

Table 1
Strong ground motion records used as input to adjacent buildings.

Earthquake (record)	Date	Soil class	Station	PGA (g)	M	D_{ss} (km)	t_d (s)	Energy E^* (m^2/s$^{1.5}$)
Aqaba (NS)	11.22.1995	NA, NA	Eilat	0.09	7.1	93.8	60	6.25
Loma Prieta (000)	10.18.1989	D, C	58223 SF Intern. Airport	0.24	6.9	64.4	40	4.86
El-Centro (180)	05.19.1940	D, C	117 El-Centro	0.34	7.2	8.3	53	3.85
Kocaeli (090)	08.17.1999	B, B	Sakarya	0.37	7.4	3.1	60	4.33
Loma Prieta (090)	10.18.1989	B, B	Corralitos	0.48	7.1	5.1	40	4.15
Loma Prieta (285)	10.18.1989	A, NA	Coyote Lake Dam	0.48	7.1	21.8	40	3.17
Northridge (052)	06.18.1994	D, C	74 Sylmar	0.61	6.7	6.2	40	4.92
Loma Prieta (090)	10.18.1989	D, NA	14 WAHO	0.63	7.1	16.9	25	4.33
Kobe (000)	01.16.1995	B, B	0 KJMA	0.82	6.9	0.6	48	4.30
Northridge (360)	01.17.1994	C, C	77 Rinaldi Receiving St.	0.84	6.7	7.1	15	4.05
Chi-Chi (W)	09.20.1999	2, C	TCU129	1.01	7.6	1.18	90	4.82
San Fernando (254)	02.09.1971	B, NA	279 Pacoima Dam	1.20	6.6	2.8	40	3.00

Soil class = geomatrix soil class, USGS, NA = not available, PGA = peak ground acceleration, M = magnitude, D_{ss} = site–source distance, t_d = earthquake total duration, $E = \sqrt{\int_0^{t_d}\ddot{u}_g^2(t)dt}$ [47].

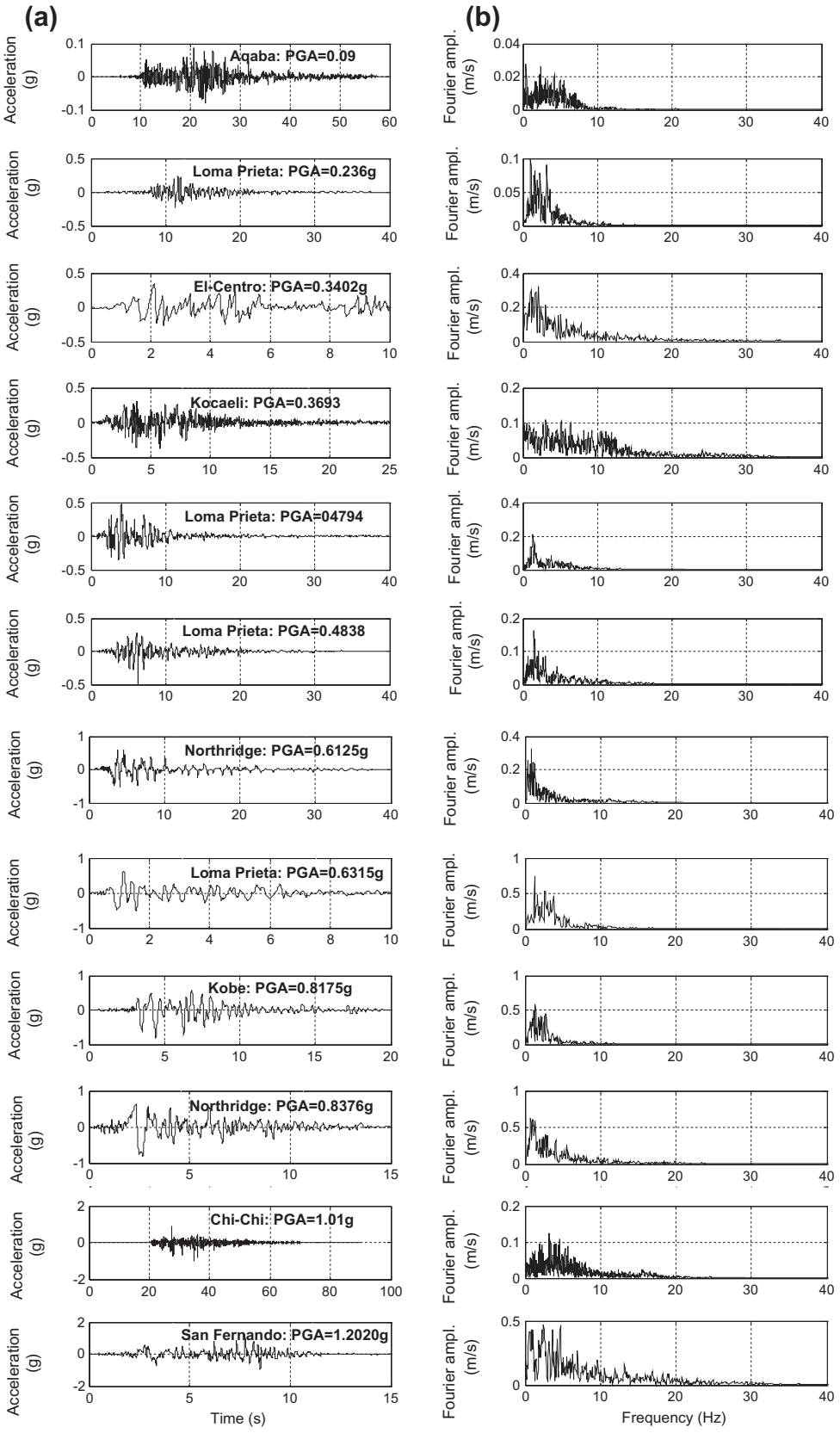

Fig. 3. Input ground motion to adjacent buildings (a) acceleration and (b) Fourier amplitude (see Table 1).

Table 2
Maximum inelastic response quantities for adjacent buildings with fixed-base under different ground motion inputs.

Earthquake	Structure on left									Structure on right									f_P (kN)
	μ	DI_{PA}	DI_{AP}	DI_{FC}	DI_H	E_I (kN m)	E_D (kN m)	E_H (kN m)	E_P (kN m)	μ	DI_{PA}	DI_{AP}	DI_{FC}	DI_H	E_I (kN m)	E_D (kN m)	E_H (kN m)	E_P (kN m)	
Aqaba (NS)	2.41	1.03	0.28	0.84	0.64	62.26	38.22	38.21	4.85	2.83	2.10	0.37	2.48	0.52	4327.10	2490.20	1959.40	10.57	1136.40[2]
Loma Prieta (000)	2.41	1.18	0.28	1.14	0.67	85.04	42.67	51.91	0.20	3.90	2.89	0.58	3.03	0.72	3932.60	1485.40	2391.70	8.99	1758.80[2]
El-Centro (180)	4.79	1.66	0.76	1.21	0.68	82.24	28.57	55.15	3.4	1.87	0.85	0.20	0.76	0.65	1298.10	633.58	597.95	6.77	607.30[1]
Kocaeli (090)	1.99	0.54	0.20	0.27	0.41	25.06	20.46	12.47	2.51	2.35	0.97	0.27	0.89	0.63	1474.60	857.67	703.52	7.87	1834.10[2]
Loma Prieta (090)	2.70	0.96	0.34	0.84	0.64	66.58	37.00	38.07	2.57	1.55	0.71	0.20	0.72	0.64	1216.90	664.75	565.54	6.77	1632.40[1]
Loma Prieta (285)	2.74	0.72	0.35	0.39	0.59	38.32	25.08	17.98	3.03	1.98	0.52	0.20	0.26	0.50	635.33	409.69	205.22	5.07	1066.80[1]
Northridge (052)	6.21	3.02	1.04	2.96	0.72	209.33	71.15	134.92	6.27	1.63	0.66	0.20	0.52	0.59	1026.33	608.94	407.85	3.43	1325.30[1]
Loma Prieta (090)	4.31	1.21	0.66	0.66	0.54	33.81	22.18	30.14	13.07	2.54	1.24	0.31	1.19	0.86	1586.30	611.05	935.89	22.92	2580.60[1]
Kobe (000)	5.29	1.99	0.86	1.56	0.74	99.49	36.30	71.22	1.07	2.18	1.43	0.24	1.47	0.76	2004.40	763.95	1160.20	13.43	2822.90[1]
Northridge (360)	8.28	3.11	1.46	2.42	0.87	150.92	49.47	110.09	7.62	6.05	1.80	1.01	1.16	0.87	1592.40	644.09	914.25	24.20	5171.70[1]
Chi-Chi (EW)	1.67	0.39	0.20	0.14	0.66	17.92	18.37	6.52	9.65	2.00	0.67	0.20	0.54	0.57	1811.80	1464.20	427.58	1.01	1655.50[1]
San Fernando (254)	1.68	0.44	0.20	0.22	0.75	30.00	12.99	9.94	8.80	1.36	0.45	0.20	0.31	0.34	865.64	655.87	243.54	0.67	2314.00[1]

$u_{yl} = 0.067$ m, $u_{yr} = 0.011$ m, $\mu_{u1} = 6$, $\mu_{ur} = 6$, $\gamma = 0.15$, $d = 0.05$ m, μ = maximum ductility, DI_{PA} = Park and Ang damage index, DI_{FC} = Fajfar and Cosenza damage index, DI_{AP} = Allahabadi and Powell damage index, f_P = Pounding force, DI_H = hysteretic damage index, E_I = maximum input energy, E_D = maximum damping energy, E_H = maximum yielding energy, E_P = maximum pounding energy. The superscript on the numerical value of the pounding force in last column indicates how many times pounding occurs.

5. Numerical results and discussion

This section provides numerical illustrations of the formulation developed in this paper for fixed-base adjacent buildings (Section 5.1) and for isolated-base adjacent buildings (Section 5.2).

5.1. Fixed-base adjacent buildings

In the numerical analysis, all acceleration records have been scaled to 0.50g PGA to ensure inelastic response of structures and the separation distance d is taken equal to 0.05 m. The separation distance is changed later to examine its effect on the response of adjacent buildings. The parameters of the damage indices are taken as $\mu_{u_l} = \mu_{u_r} = 6.0$, and $\gamma = 0.15$ (see Fig. 1 and Eqs. (1–4)). The system parameters and yield strength of adjacent buildings are as provided in Section 4.1. The structural response of both buildings is calculated using Newmark-β method in the Matlab platform ($\alpha = 0.25$, $\beta = 0.50$ and $\Delta t = 0.005$ s).

The numerical results for fixed-base buildings are presented in Table 2 and Figs. 4–9. Table 2 summarizes the numerical values for the maximum ductility demand μ, Park and Ang damage index (DI_{PA}), Fajfar and Cosenza damage index (DI_{CF}), Powell and Allahabadi damage index (DI_{AP}), the hysteretic damage index (DI_H), the pounding force f_1, the maximum input energy E_I, the maximum damping energy E_D, the maximum yield energy E_H and the maximum pounding energy E_P for the considered two buildings during collisions.

Pounding of fixed-base adjacent buildings is seen to occur once or twice (see Table 2). Note that superscript on the numerical values of the pounding force in Table 2 indicates the number of

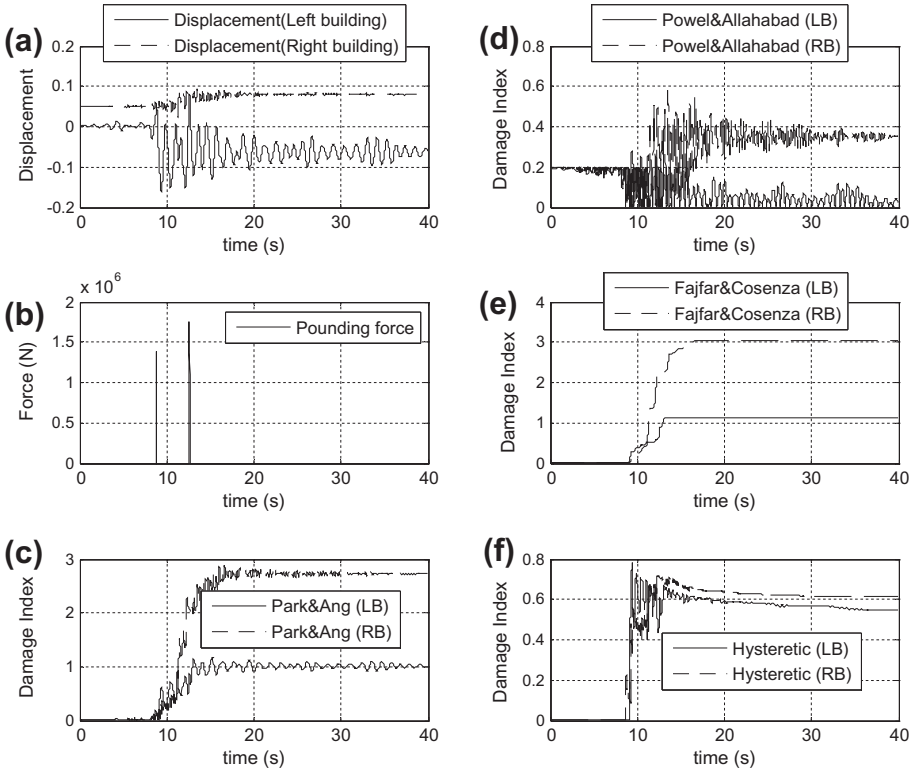

Fig. 4. Response parameters for fixed-base buildings to Loma Prieta record (000) (a) Displacements, (b) pounding force, (c) Park and Ang damage index, (d) Powell and Allahabadi damage index, (e) Fajfar and Cosenza damage index, and (f) damage index based on hysteric energy.

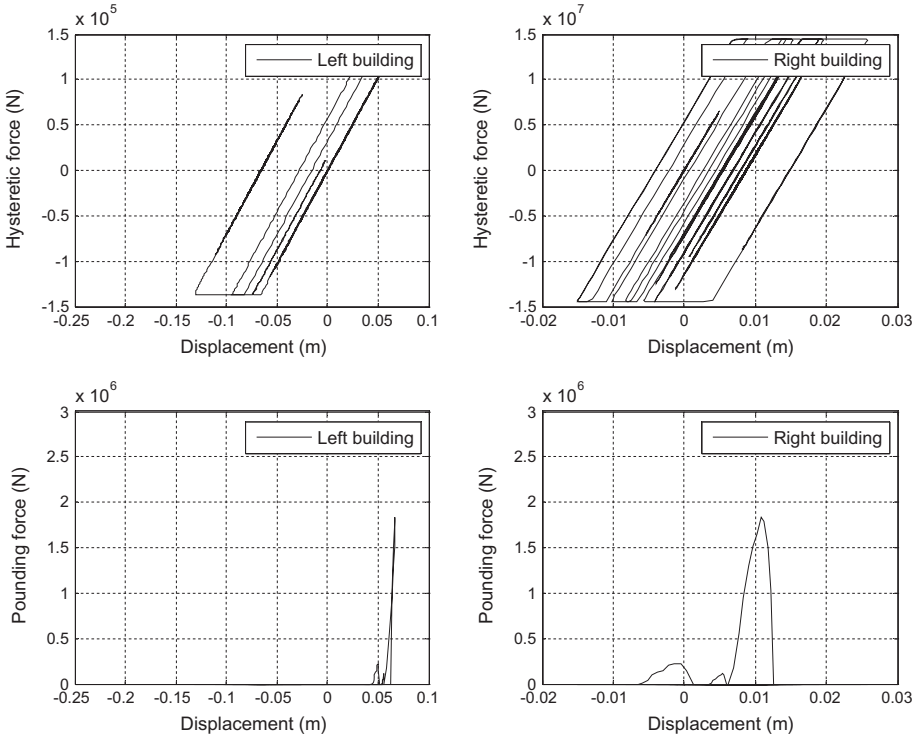

Fig. 5. Hysteretic and pounding forces for fixed-base buildings under Kocaeli record.

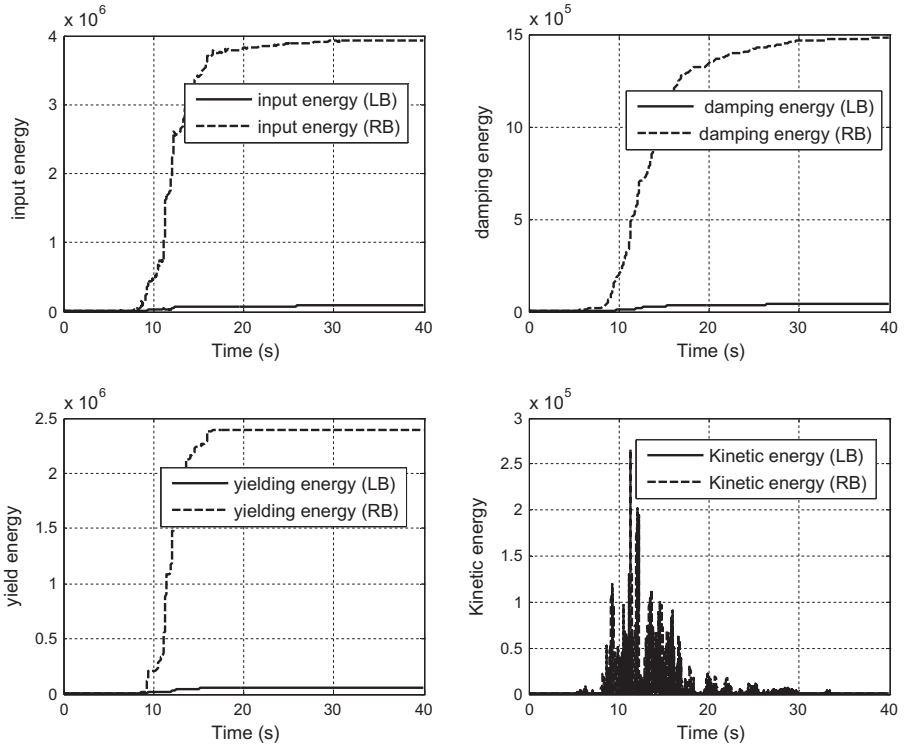

Fig. 6. Input and dissipated energy for adjacent fixed-base buildings under Loma Prieta earthquake records (far fault).

occurrence of pounding of adjacent buildings. It can be seen that acceleration records from El Centro 1940 earthquake, Northridge 1989 earthquake and 1995 Kobe earthquake produce high ductility demands and large damage indices (see Table 2). This could be attributed to the characteristics of these records since some of these records have rich frequency content, high energy and small source-site distance (near-fault records). Note also that these three earthquakes are measured on *D*, *C* and *B* soil classes, respectively. The input and dissipated energies from the first three earthquakes are relatively high compared to those from the last two

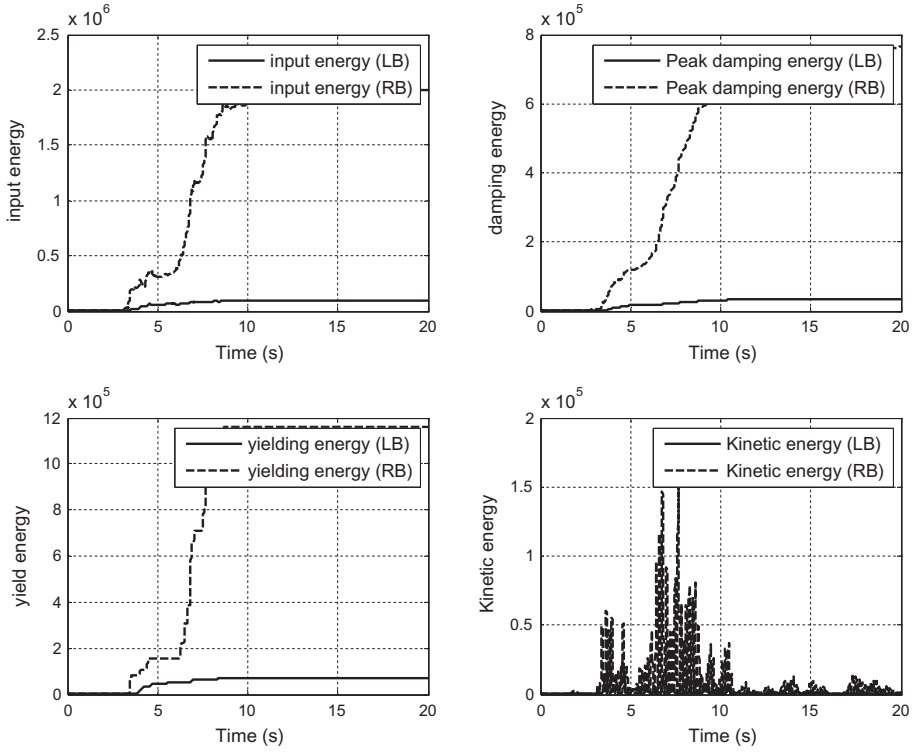

Fig. 7. Input and dissipated energy for adjacent fixed-base buildings under Kobe earthquake records (near fault).

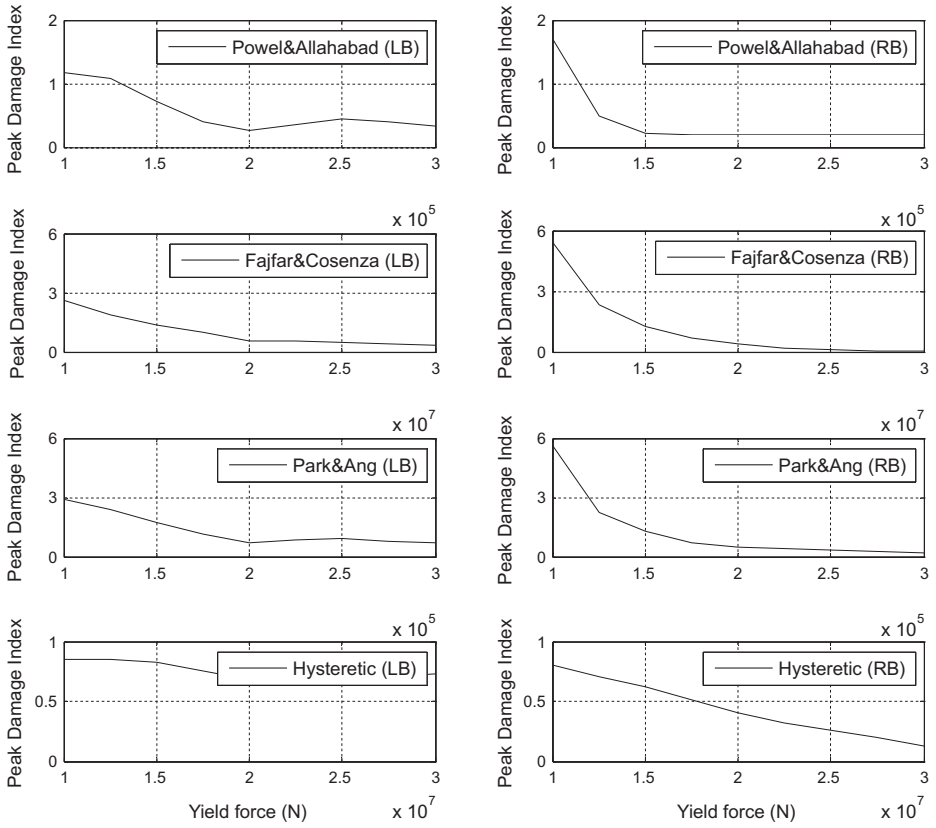

Fig. 8. Influence of yield force on damage indices of adjacent fixed-base buildings under Kobe earthquake (d = 0.05 m).

earthquakes. In fact, according to the numerical values of Park and Ang damage index for the first three earthquakes, both buildings are totally collapsed (see Table 2). Furthermore, other earthquake records such as 1999 Chi-Chi and 1971 San Fernando and 1999 Kocaeli produce lower ductility demands and lower damage indices (either repairable damage or damaged beyond repair but total collapse does not occur). We now focus our attention on the influence of the structure's properties on the ductility demands,

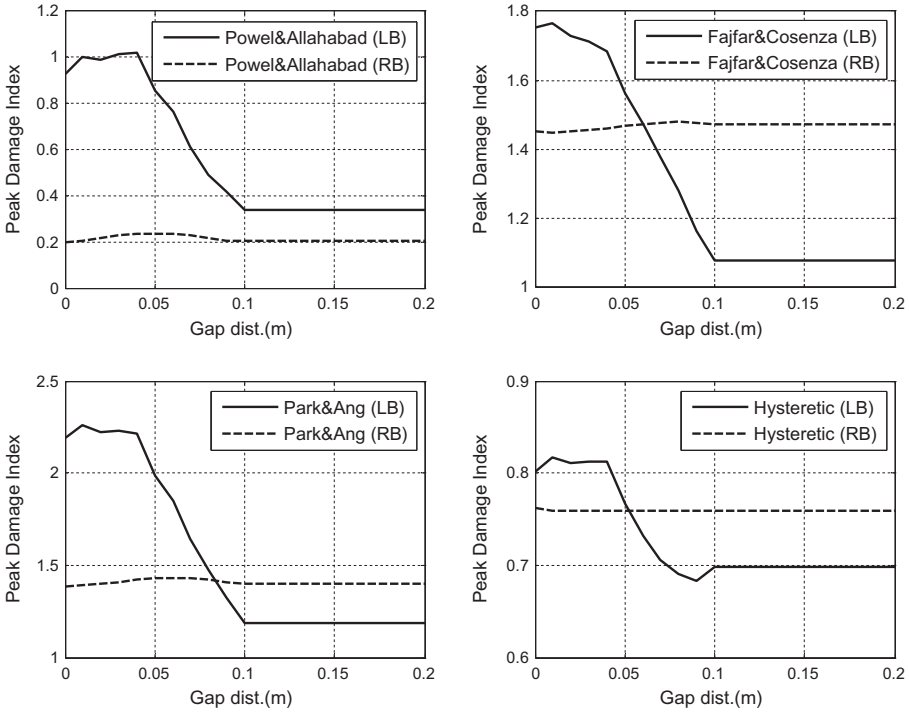

Fig. 9. Influence of separation distance between adjacent fixed-base buildings on damage indices under Kobe earthquake.

Table 3
Maximum inelastic response quantities for adjacent buildings with isolated-base under different ground motion inputs.

Earthquake	Structure on left									Structure on right									f_P (kN)
	μ	DI_{PA}	DI_{AP}	DI_{FC}	DI_H	E_I (kN m)	E_D (kN m)	E_H (kN m)	E_P (kN m)	μ	DI_{PA}	DI_{AP}	DI_{FC}	DI_H	E_I (kN m)	E_D (kN m)	E_H (kN m)	E_P (kN m)	
Aqaba (NS)	4.03	1.75	0.61	1.62	0.70	19.94	41.15	73.66	2.27	1.35	0.28	0.20	0.07	0.12	327.49	581.68	56.05	2.80	1316.70[3]
Loma Prieta (000)	5.72	1.80	0.94	1.61	0.53	21.43	37.48	73.12	32.92	8.96	2.92	1.59	1.90	0.79	887.36	744.37	1500.3	3.49	2805.70[2]
El-Centro (180)	5.84	1.90	0.97	1.26	0.51	20.38	28.03	57.53	30.12	2.71	1.14	0.34	1.26	0.82	424.68	446.11	992.22	21.37	3607.80[1]
Kocaeli (090)	3.73	1.03	0.55	0.54	0.63	12.51	13.69	24.92	1.51	1.66	0.38	0.20	0.17	0.71	210.22	131.52	133.55	3.57	2534.00[4]
Loma Prieta (090)	4.54	1.39	0.71	0.85	0.40	54.74	27.86	38.55	33.42	4.53	2.90	0.71	3.06	0.80	488.10	884.97	2414.70	0.50	2176.40[2]
Loma Prieta (285)	2.71	0.71	0.34	0.38	0.42	27.26	12.63	17.52	13.74	2.00	0.48	0.20	0.19	0.76	137.09	245.20	157.38	0.33	1367.40[2]
Northridge (052)	6.67	2.71	1.13	2.31	0.71	82.74	36.08	105.37	9.72	12.92	5.94	2.38	5.34	0.86	2119.20	1217.6	4216.6	11.72	1477.30[1]
Loma Prieta (090)	1.69	0.41	0.20	0.23	0.57	41.99	12.85	10.51	1.11	2.39	0.61	0.28	0.37	0.83	580.87	300.58	289.24	1.08	1191.90[1]
Kobe (000)	4.29	1.39	0.66	1.45	0.65	37.40	32.91	66.27	9.90	8.43	3.43	1.49	3.23	0.84	1078.70	940.97	2554.50	7.87	2225.00[1]
Northridge (360)	4.06	2.25	0.61	2.17	0.84	57.50	43.40	99.03	20.92	11.07	3.94	2.01	3.17	0.85	1859.00	961.57	2505.60	3.89	3803.50[1]
Chi-Chi (EW)	3.78	2.90	0.55	3.08	0.58	39.57	66.97	140.25	24.90	15.55	8.26	2.91	7.56	0.78	2384.90	1845.90	5970.50	11.21	2503.40[2]
San Fernando (254)	3.20	0.99	0.44	0.62	0.79	22.47	15.32	28.46	8.76	2.61	0.68	0.32	0.32	0.86	207.15	91.86	255.00	7.48	3159.20[1]

u_{yl} = 0.067 m, u_{yr} = 0.011 m, μ_{u1} = 6, μ_{ur} = 6, γ = 0.15, d = 0.05 m, μ = maximum ductility, DI_{PA} = Park and Ang damage index, DI_{FC} = Fajfar and Cosenza damage index, DI_{AP} = Allahabadi and Powell damage index, f_P = Pounding force, DI_H = hysteretic damage index, E_I = maximum input energy, E_D = maximum damping energy, E_H = maximum yielding energy, E_P = maximum pounding energy. The superscript on the numerical value of the pounding force in last column indicates how many times pounding occurs.

dissipated energies, and associated damage indices. Referring to Figs. 6 and 7 and Table 2, for the same input ground motion, it can be seen that the building on right (stiff structure) has higher ductility demand and large damage index compared to the building on left (flexible building). This is because the displacement demand for stiff structure is larger than that for the flexible structure. Additionally, it may be recalled that the peak pounding force follows the same trend as the peak acceleration of the flexible and lighter building [11].

Fig. 4 shows the response quantities for left and right buildings under Loma Prieta earthquake record. Specifically, this figure depicts the displacement, pounding force and damage indices in time domain for both buildings. Note that pounding occurs between the two buildings twice for a very short time duration which is seen in the displacement plot where displacements of left and right buildings intersect. The plot of the pounding force implies also that pounding starts at the same time instant and lasts for a very short duration of time. Notice that the pounding force is the same quantity for both buildings. However, its effect on each building may be different (recall that the left building is flexible while the right building is rigid and that the two buildings have different responses under the same earthquake). With this in mind, we show the hysteretic loops (hysteretic force versus displacement) and the pounding loops (pounding force versus displacement) for both buildings under the 1999 Kocaeli ground acceleration in Fig. 5. The figure reflects the fact that the building on right has more hysteretic loops and more dissipated hysteretic energy compared to the building on left. It can be noticed also that the pounding loops for the building on right is wider compared to that on left. This observation is supported by the higher values of ductility factor and damage index for the building on right compared to the same quantities for the building on left (see Table 2). For instant,

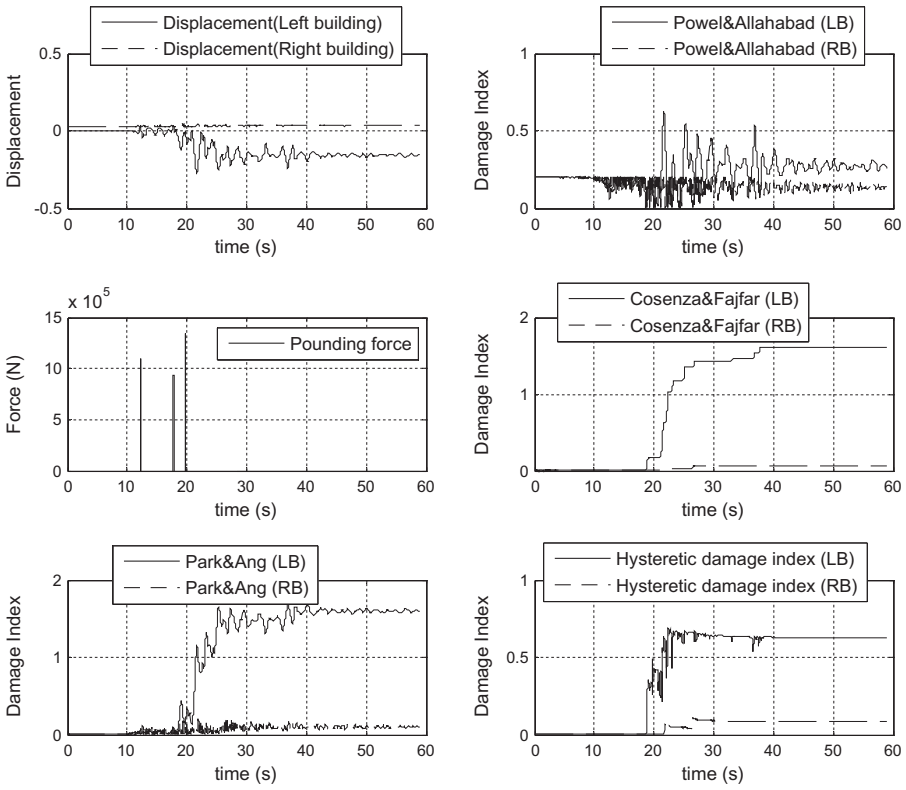

Fig. 10. Response parameters for isolated-base buildings to Aqaba record (a) Displacements, (b) pounding force, (c) Park and Ang damage index, (d) Powell and Allahabadi damage index, (e) Fajfar and Cosenza damage index, and (f) damage index based on hysteric energy.

$\mu = 1.99$, $DI_{PA} = 0.54$, $DI_{AP} = 0.20$, $DI_{FC} = 0.27$, $DI_H = 0.41$ for the left building while $\mu = 2.35$, $DI_{PA} = 0.97$, $DI_{AP} = 0.27$, $DI_{FC} = 0.89$, $DI_H = 0.63$ for right building. Note that, according to Park and Ang damage criterion, the left building experiences unrepairable damage while the right building is fully collapsed. The numerical values of the pounding and the hysteretic energies listed in Table 2 support the same observation. In fact, the numerical values of energies given in Table 2 reflect that the hysteretic energy is substantially higher than the pounding energy which can be expected given that pounding occurs for short durations (note that for a sufficiently large separation distance pounding may not occur leading to zero pounding force and zero pounding energy). The same fact is also reflected in the input and dissipated energies for both buildings where those for left building are $E_I = 25.06$ kN m, $E_D = 20.46$ kN m and $E_H = 12.17$ kN m while those for the right building are $E_I = 1474.60$ kN m, $E_D = 857.67$ kN m and $E_H = 703.52$ kN m.

Figs. 6 and 7 show the input energy and dissipated (yielding, damping and kinetic) energy for the fixed-base adjacent buildings under the Loma Prieta earthquake record (far-fault) and the Kobe earthquake record (near-fault), respectively. For the given structures and separation distance, it has been observed that near-fault earthquakes exert less input energy on adjacent structures than far-fault earthquakes (see Table 2). Consequently, adjacent buildings dissipate less energy under near-fault earthquakes compared with far fault earthquakes. In both cases, however, the input energy to both structures is dissipated mainly by yielding and damping mechanisms. The strain and kinetic energies are very small compared to the yield and damping energies. The kinetic energy reaches its maximum value during the strong phase of the ground acceleration and diminishes by the end of the ground shaking.

To investigate the effect of the yield strength of adjacent buildings on the associated structural damage, the yield strength of both buildings was changed, keeping all other parameters unchanged, and the dynamic analysis of both structures was carried out in each case. Fig. 8 depicts the influence of the yield force on damage indices of both buildings. It can be observed that all damage indices decrease when the yield strength increases. The decrease in the damage indices of the right building is higher than that of the left building.

To examine the effect of the separation distance on peak response quantities of adjacent buildings, the value of the gap distance between adjacent buildings (d) is varied between 0 and 0.20 m and the peak response of both buildings is determined for each separation distance. Fig. 9 shows the peak damage indices for both buildings under the 1995 Kobe earthquake. It is seen that the separation distance has substantial influence on the peak response of both buildings. For example, the peak damage indices increase when the separation distance decreases. Pounding does not occur between adjacent buildings for a separation distance of about 0.10 m where the damage indices for adjacent buildings stabilize and approach constant values (see Figs. 9 and 10). This, in turn, implies that the damage index for both buildings does not include contribution from pounding since the pounding force between the two buildings vanishes. Furthermore, the energy resulting from pounding effects diminishes.

5.2. Isolated-base adjacent buildings

The set of 12 earthquake records used for fixed-base buildings is also adopted here as input to dynamic analysis of adjacent buildings with isolated-base and all records are scaled to 0.50g PGA. The separation distance is taken as $d = 0.05$ m which is changed later to study its effect on pounding and damage of adjacent buildings. The structures parameters are taken the same as in the fixed-base buildings, but with the important difference that both

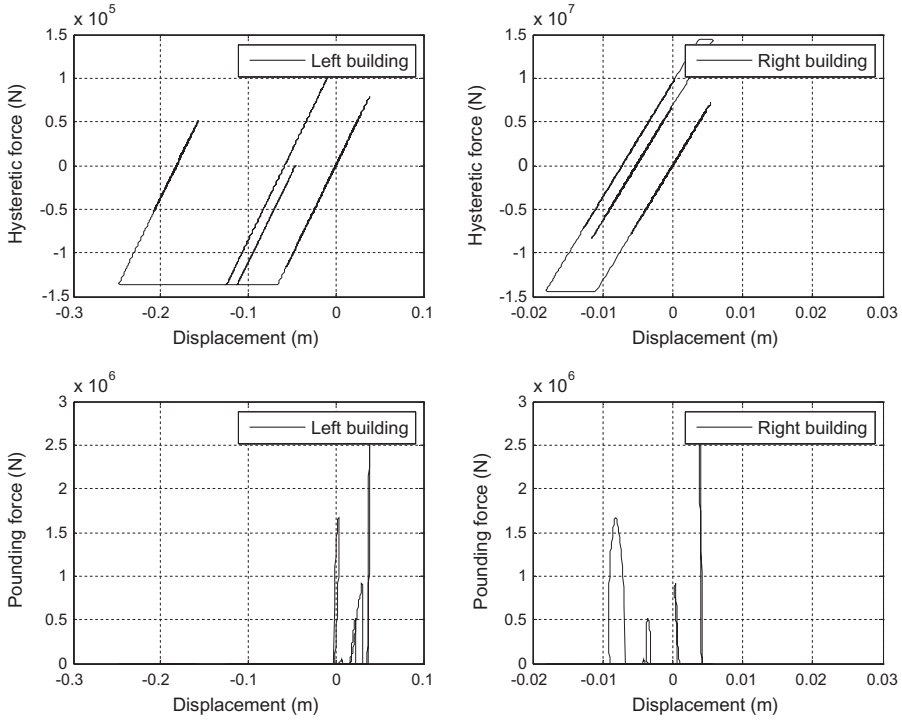

Fig. 11. Hysteretic and pounding forces for isolated-base buildings under Kocaeli record.

structures are supported on isolated-bases (see Fig. 2 and Sections 3.1.2 and 5).

The results on the structural response for base-isolated adjacent buildings are presented in Table 3 and Figs. 10–13. Table 3 summarizes the numerical values for the maximum ductility demand μ, Park and Ang damage index (DI_{PA}), Fajfar and Cosenza damage index (DI_{CF}), Powell and Allahabadi damage index (DI_{AP}), the hysteretic damage index (DI_H), the pounding force f_1, the maximum input energy E_I, the maximum damping energy E_D, the maximum yield energy E_H and the maximum pounding energy E_P for the two adjacent buildings. Fig. 10 shows the response quantities for both buildings (displacements and damage indices) for left and right buildings to the 1995 Aqaba record. Fig. 11 depicts the plots of the hysteretic and the pounding forces as functions of the displacements for both buildings under the 1999 Kocaeli record. Figs. 12 and 13 show the influence of the separation distance on the peak

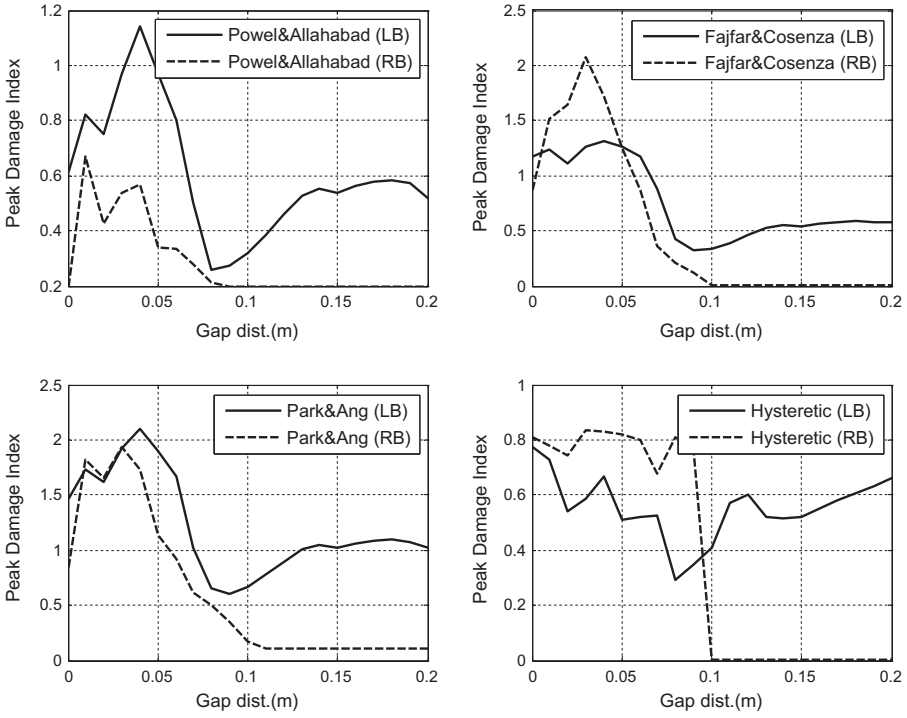

Fig. 12. Influence of separation distance between adjacent isolated-base buildings on damage indices under El Centro earthquake.

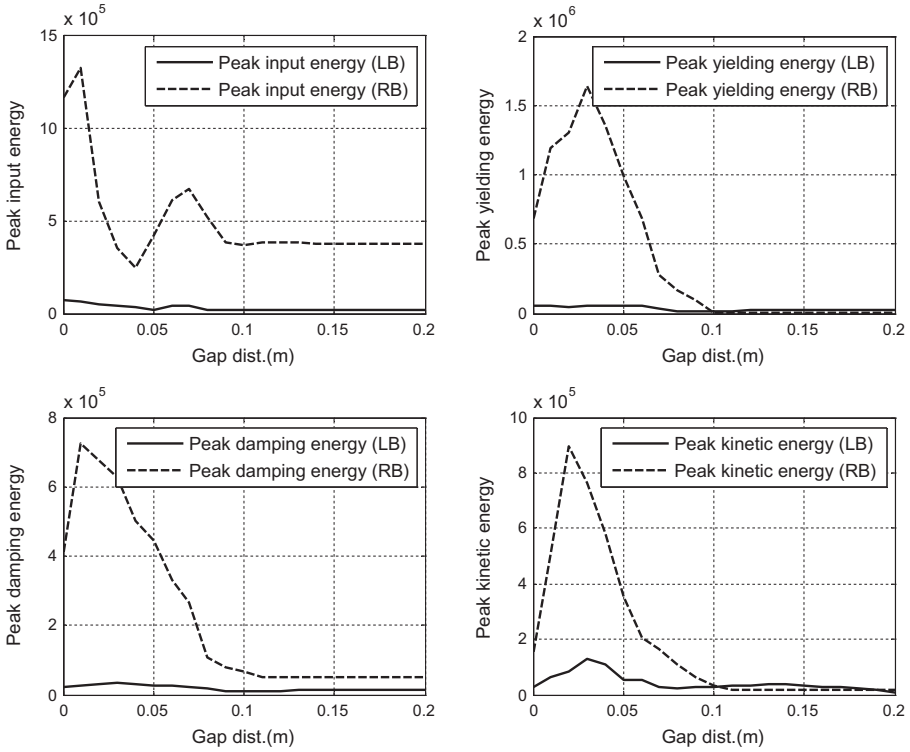

Fig. 13. Influence of separation distance between adjacent isolated-base buildings on input, damping, hysteretic and kinetic energies under El Centro earthquake.

damage indices and peak input, damping, hysteretic, and kinetic energies to the 1940 El Centro record. The numerical results presented in these figures and Table 3 reveals that adjacent base-isolated structures respond differently to earthquake loads from fixed-base adjacent buildings. For instant, under the 1940 El Centro record the ductility factor, Park and Ang damage index are 5.84, 1.90 and 4.79, 1.66 for base-isolated and fixed-base left buildings, respectively. Furthermore, pounding of adjacent structures with isolated-bases occurs several times (see Table 3). This could be attributed to the fact that base-isolated buildings are more flexible than fixed-base buildings. Additionally, for the structures considered, the maximum pounding forces are higher for the base-isolated buildings than for the fixed-base buildings. Fig. 12 indicates that pounding of base-isolated buildings occurs at a wider displacement range compared to fixed-base buildings (see Fig. 10).

6. Conclusions

Damage assessment of adjacent buildings under earthquake loads is studied in this paper. Earlier studies on response analysis of adjacent buildings under earthquake loads have focused on pounding effect in terms of displacement, velocity and acceleration and associated pounding force. This study explores the ductility, pounding force, input energy and dissipated energy by damping and yielding and damage indices in neighboring buildings caused by earthquake loads. Damage indices include those developed by Park and Ang, Fajfar and Cosenza, Allahabadi and Powell and the damage index estimated based on hysteretic energy dissipated by yielding. These response parameters are believed to be of significant importance in assessing damage of adjacent buildings since they provide a quantitative measure of damage level and thus a decision on necessary repair can be taken. For instant, the inelastic displacement of both structures may not provide an efficient measure of the structural performance compared to damage indices which provide a quantitative measure of the structural performance. Additionally, this study has investigated the influence of the separation distance between adjacent buildings and the yield strength of both buildings on the associated structural response and damage indices. It has been found that damage indices increase as the separation distance decreases due to the effect resulting from the pounding force between adjacent buildings. Additionally, adjacent buildings with fixed-bases have been seen to respond differently from adjacent buildings with isolated-bases. In current study, pounding of fixed-base buildings occurs once or twice compared to isolated-base adjacent buildings in which pounding occurs between one and four times. Furthermore, fixed-base adjacent buildings dissipate larger energy by hysteretic mechanism compared to isolated-base adjacent buildings which dissipate less hysteretic energy. This could be attributed to the fact that isolated-base buildings are more flexible structures compared to fixed-base buildings.

In the present study, pounding of simple structures of equal height modeled as SDOF systems with elastic–plastic force–deformation relationship is studied. Future research work will focus on investigating damage of adjacent MDOF structures of different heights with degrading nonlinear models, accounting for formation of plastic hinges. In this case, a weighted summation of local damage indices of individual structural members can be used as an estimate of the global damage index for the structure. Additionally, examining the damage of adjacent buildings under probabilistic ground motion inputs is also of significant interest to structural engineers and will be considered in a future study.

Acknowledgements

This research paper was funded by the Deanship of Scientific Research (DSR), King Abdulaziz University, Jeddah, under Grant

No. 9-829-D1432. The authors, therefore, acknowledge with thanks DSR technical and financial support.

References

[1] Moustafa A, editor. Earthquake-resistant structures: design, assessment and rehabilitation. Croatia: InTech; 2012.
[2] Comartin C, Brzev S, Naeim F, Greene F, Blondet M, Cherry S, et al. A challenge to earthquake engineering professionals. Earthq Spect 2004;20(4):1049–56.
[3] USGS/EERI. The Mw 7.0 Haiti earthquake of January 12, 2010: USGS/EERI Advance Reconnaissance Team, TEAM Report V. 1.1; February 23, 2010.
[4] Takewaki I, Murakami S, Fujita K, Yoshitomi S, Tsuji M. The 2011 off the Pacific coast of Tohoku earthquake and response of high-rise buildings under long-period ground motions. Soil Dyn Earthq Eng 2011;31(11):1511–28.
[5] Moustafa A. Damage-based design earthquake loads for single-degree-of-freedom inelastic structures. ASCE J Struct Eng 2011;137(3):456–67.
[6] Moustafa A, Takewaki I. Characterization and modeling of near-fault pulse-like strong ground motion via damage-based critical excitation method. Struct Eng Mech 2010;34(6):755–78.
[7] Moustafa A. Seismicity of Egypt and national seismic network. In: Proceedings of thirteenth international conference on structural and geotechnical engineering, Cairo, Egypt; 2009. p. 27–9.
[8] Rosenbluth E, Meli R. The 1985 earthquake: causes and effects in Mexico City. Concr Int (ACI) 1986;8:23–36.
[9] Anagnostopoulos SA. Pounding of buildings in series during earthquakes. Earthq Eng Struct Dyn 1988;16(3):443–56.
[10] Jankowski R. Non-linear FEM analysis of pounding-involved response of buildings under non-uniform earthquake excitation. Eng Struct 2012;37:99–105.
[11] Karayannis CG, Favvata MJ. Earthquake-induced interaction between adjacent reinforced concrete structures with non-equal height. Earthq Eng Struct Dyn 2005;34(1):1–20.
[12] Komodromos P, Polycarpou PC, Papaloizou L, Phocas MC. Response of seismically isolated buildings considering poundings. Earthq Eng Struct Dyn 2007;36(12):1605–22.
[13] Anagnostopoulos SA, Karamaneas CE. Use of collision shear walls to minimize seismic separation and to protect adjacent buildings from collapse due to earthquake-induced pounding. Earthq Eng Struct Dyn 2008;37(12):1371–88.
[14] Jankowski R. Non-linear FEM analysis of earthquake-induced pounding between the main building and the stairway tower of the Olive View Hospital. Eng Struct 2009;31(8):1851–64.
[15] Mahmoud S, Jankowski R. Pounding-involved response of isolated and non-isolated buildings under earthquake excitation. Earthq Struct 2010;1(3):3250–62.
[16] Jankowski R, Wilde K, Fujino Y. Pounding of superstructure segments in isolated elevated bridge during earthquakes. Earthq Eng Struct Dyn 1998;27(5):487–502.
[17] Kasai K, Maison BF. Building pounding damage during the 1989 Loma Prieta earthquake. Eng Struct 1997;19(3):195–207.
[18] Mahmoud S, Jankowski R. Elastic and inelastic multi-storey buildings under earthquake excitation with the effect of pounding. J Appl Sci 2009;9(18):3250–62.
[19] Maison BF, Wei Kasai K. Dynamics of pounding when two buildings collide. Earthq Eng Struct Dyn 1992;21(9):771–86.
[20] Chau KT, Wei XX. Pounding of structures modelled as nonlinear impacts of two oscillators. Earthq Eng Struct Dyn 2001;30(5):633–51.
[21] Chau KT, Wei XX, Guo X, Shen CY. Experimental and theoretical simulation of seismic poundings between two adjacent structures. Earthq Eng Struct Dyn. 2003;32(4):537–54.
[22] Tsai HC. Dynamics analysis of base-isolated shear beams bumping against stops. Earthq Eng Struct Dyn 1997;26(5):515–28.
[23] Malhotra PK. Dynamics of seismic impacts in base-isolated buildings. Earthq Eng Struct Dyn 1997;26(8):797–813.
[24] Dimova SL. Numerical problems in modelling of collision in sliding systems subjected to seismic excitations. Adv Eng Softw 2000;31(7):467–71.
[25] Nagarajaiah S, Sun X. Base-isolated FCC building: impact response in Northridge earthquake. J Struct Eng 2001;127(9):1063–75.
[26] Athanassiadou CJ, Penelis GG. Elastic and inelastic system interaction under an earthquake motion. In: Proceedings of the 7th Hellenic conference on concrete, Patras, Greece; 1985. p. 211–6.
[27] Pantelides CP, Ma X. Linear and nonlinear pounding of structural systems. Comput Struct 1998;66(1):79–92.
[28] Muthukumar S, DesRoches R. A Hertz contact model with nonlinear damping for pounding simulation. Earthq Eng Struct Dyn 2006;35(7):811–28.
[29] Jankowski R. Pounding force response spectrum under earthquake excitation. Eng Struct 2006;28(8):1149–61.
[30] Jankowski R. Earthquake-induced pounding between equal height buildings with substantially different dynamic properties. Eng Struct 2008;30(10):2818–29.
[31] Polycarpou PC, Komodromos P. Earthquake-induced poundings of a seismically isolated building with adjacent structures. Eng Struct 2010;32(7):1937–51.
[32] Agarwal VK, Niedzwecki JM, van de Lindt JW. Earthquake induced pounding in friction varying base isolated buildings. Eng Struct 2007;29(11):2825–32.
[33] Fajfar P. Equivalent ductility factors, taking into account low-cyclic fatigue. Earthq Eng Struct Dyn 1992;21(10):837–48.
[34] Cosenza C, Manfredi G, Ramasco R. The use of damage functionals in earthquake engineering: a comparison between different methods. Earthq Eng Struct Dyn 1993;22(10):855–68.
[35] Ghobarah A, Abou-Elfath H, Biddah A. Response-based damage assessment of structures. Earthq Eng Struct Dyn 1999;28(1):79–104.
[36] Poljanšek K, Fajfar P. A new damage assessment of reinforced concrete frame structures. In: The 14th world conference on earthquake engineering; 2008.
[37] Wang J, Chi-Chang Lin C, Yen S. A story damage index of seismically-excited buildings based on modal frequency and mode shape. Eng Struct 2007;29(9):2143–57.
[38] Zapico JL, González MP. Numerical simulation of a method for seismic damage identification in buildings. Eng Struct 2006;28(2):255–63.
[39] Powell GH, Allahabadi R. Seismic damage predictions by deterministic methods: concepts and procedures. Earthq Eng Struct Dyn 1988;16(5):719–34.
[40] Park YJ, Ang AHS. Mechanistic seismic damage model for reinforced concrete. ASCE J Struct Eng 1985;111(4):722–39.
[41] Park YJ, Ang AHS, Wen YK. Seismic damage analysis of reinforced concrete buildings. ASCE J Struct Eng 1985;111(4):740–57.
[42] Park YJ, Ang AHS, Wen YK. Damage-limiting aseismic design of buildings. Earthq Spect 1987;3(1):1–26.
[43] Jankowski R. Nonlinear rate dependent model of high damping rubber bearing. Bull Earthq Eng 2003;1(3):397–403.
[44] Chopra AK. Dynamics of structures. 3rd ed. New York: Prentice Hall; 2006.
[45] Jankowski R. Non-linear viscoelastic modelling of earthquake-induced structural pounding. Earthq Eng Struct Dyn 2005;34(6):595–611.
[46] Jankowski R. Analytical expression between the impact damping ratio and the coefficient of restitution in the nonlinear viscoelastic model of structural pounding. Earthq Eng Struct Dyn 2006;35(4):517–24.
[47] Arias A. A measure of earthquake intensity: seismic design of nuclear power plants. Cambridge, MA: MIT press; 1970. p. 438–68.
[48] Zahrah TF, Hall WJ. Earthquake energy absorption in SDOF structures. J Struct Eng 1984;110(8):1757–72.
[49] Uang C-M, Bertero VV. Evaluation of seismic energy in structures. Earthq Eng Struc Dyn 1990;19(1):77–90.
[50] Abbas AM. Critical earthquake load inputs for simple inelastic structures. J Sound Vib 2006;296(4–5):949–67.